The Effect of Excimer Laser Treatment on the Surface Roughness and Fracture Strength of Alumina Substrates

Federal Manufacturing & Technologies

J. E. Smoot

KCP-613-6070

Published May 1998

Final Report

AlliedSignal Prepared Under Contract Number DE-ACO4-76-DP00613 for the United States Department of Energy

DISCLAIMER

AlliedSignal Inc.

Federal Manufacturing
& Technologies

P. O. Box 419159

Kansas City, Missouri

64141-6159

A prime contractor with the United States

Department of Energy under Contract Number

DE-ACO4-76-DP00613.

KCP-613-6070

Distribution Category UC-706

Approved for public release; distribution is unlimited.

THE EFFECT OF EXCIMER LASER TREATMENT

ON THE SURFACE ROUGHNESS AND FRACTURE STRENGTH

OF ALUMINA SUBSTRATES

J. E. Smoot

Published May 1998

Final Report

J. E. Smoot, Project Leader

Project Team:

G. W. Franti

P. E. Klingsporn

R. D. Koch

W. B. Lepley

W. D. Tuohig

Contents

Illustrations

Tables

Number

Abstract

Excimer laser irradiation at 248 nm and at various angles of incidence was shown to significantly reduce surface roughness of alumina substrates, while also producing a decrease in the amount and severity of surface defects. Also, flexural strength of the substrates was found to have increased, after irradiation and a thermal sintering process. This work was in support of the Advanced Radar Program.

Summary

The microelectronics industry requires alumina substrates with exceptionally smooth surfaces and few surface defects to allow successful deposition of metallic films for reliable electronic performance. Irradiation by a 248-nm wavelength excimer laser beam (KrF) at a fluence of 125 mJ/mm^2 and at various angles of incidence is shown to significantly reduce the surface roughness of alumina substrates. However, irradiation also creates a fine particulate deposit of alumina that only partially adheres to the substrate and impedes deposition of metal films. Annealing in air between 1350^oC and 1450^oC was found to remove the particles by sintering. As-received material showed surface roughness average (R_a) mean values of 457 nm, which was reduced to 60 nm (mean) following irradiation and 71 nm (mean) following irradiation and annealing at 1350^oC. Irradiation also produced a decrease in the number and severity of surface defects. The flexural strength and Weibull modulus were both increased by laser irradiation and thermal treatment. Flexural strength went from an as-received value of 450 MPa to 560 MPa following irradiation/sintering, measured at 10% probability of failure. The Weibull modulus was increased from the as-received value of about 9, to about 13 following irradiation/sintering. It was concluded that irradiation at an angle of incidence of 60^o from perpendicular was most effective in producing a low surface roughness.

Discussion

Scope and Purpose

The microelectronics industry requires substrate materials which allow the reliable deposition of thin film microcircuits. Features such as fine conductor lines, uniform resistors, and low value polyimide capacitors require very smooth surfaces to ensure reliable performance. Polycrystalline aluminum oxide substrates (Al_2O_3, *alpha*-alumina) with greater than 99% purity and surface grain size in the range of 1-3 um are typically used for thin film applications [1,2]. Substrates can be mechanically polished to yield a roughness average (R_a) surface finish of less than 50 nm [1]. However, mechanical polishing results in many surface imperfections such as grain pullouts and scratches, which create problems for thin film microcircuits. For example, these defects can cause polyimide thin film capacitors to short out between the conductor levels.

The purpose of this research was to evaluate excimer laser processing as an alternative to mechanical polishing for the preparation of thin film alumina substrates. Sandia National Laboratories sponsored this project in support of the Advanced Radar Program.

Prior Work

Excimer Laser Systems

The excimer laser was invented in the mid 1970s and the availability of commercial models dates back only to the mid 1980s [3]. Most published research on the subject of modifying ceramics with an excimer laser is thus less than 10 years old.

Excimer lasers are a class of electronically excited molecular gas lasers that emit high intensity, short-duration (10-40 ns) pulses of ultraviolet light. Technically, excimer is an acronym for exited dimer, where the dimer is either homonuclear (Xe_2, Ar_2) or heteronuclear (KrF, XeCl) [4]. The output wavelength can be changed by simply changing the gas mixture in the laser chamber. The five most

common wavelengths and their respective gas mixtures available are:

* ArF - 193 nm

* KrCl - 222 nm

* KrF - 248 nm

* XeCl - 308 nm

* XeF - 351 nm

Choice of which gas mixture to use is dependent upon the material to be processed. For instance, most plastics are best processed with the 308-nm laser, while most inorganics, such as metals or ceramics, are best processed with the 248-nm wavelength. The reasons for this selectivity are based mostly upon the absorption characteristics of the material [5].

Ultraviolet light is usually intensely absorbed in very thin layers of a material, causing an interaction known as ablation. Ablation can be defined as material removal, usually in very thin layers, by high intensity laser radiation. There are two types of ablation: 1) photoablation of organics and 2) pyroablation, or ablation due to heating [4]. Photoablation occurs when the weak organic bonds are broken by the laser energy and the molecules are ejected away from the surface [6]. This is a non-thermal process. Pyroablation occurs when a small volume of material intensely absorbs the radiation, heating the volume of material to vaporization [4]. Although pyroablation is a thermal process, thermal effects to the bulk material are usually minimized, due to the fact that the whole process occurs so fast (10-40 ns) as to not allow much heat conduction into the bulk material. Additionally, the vaporized material increases in volume so quickly, it ejects away from the surface immediately, carrying the thermal energy with it [7].

Unique to the excimer laser is the method in which the laser beam is manipulated prior to contacting the working surface. Most lasers, such as Nd:YAG or CO_2, exit the laser cavity as a circular beam, then are simply focused down to a small spot onto the working surface. This results in a very hot spot with which to vaporize the material, sort of a light-powered blowtorch. An excimer beam exits the laser cavity as a rectangle, approximately 10 x 20 mm size. The beam can then be passed through a mask of some desired shape, then through an objective lens, to form the mask image on the work surface, usually at some demagnification factor. This process is known as imaging the laser beam, or mask projection. The shape of the image is only limited by the mask shape available.

Probably the most important processing parameter when using an excimer laser is the fluence, usually measured at the target surface. Fluence is defined as the pulse energy/area, with the units being mJ/mm^2 [8]. Fluence is also called energy density. Fluence is important during excimer laser processing because materials react differently at various fluence levels. For a reaction such as ablation to occur, the threshold fluence for that reaction must be exceeded.

Irradiation of Ceramics

Schmatjko, et al. (1988) [9] explored the change of surface properties induced by excimer laser irradiation of five different ceramic materials (Al_2O_3, ZrO_2, SiC, Si_3N_4, AlN). Laser fluences up to

200 mJ/mm^2 were investigated. The wavelength of the laser used was not mentioned. The laser was imaged through a rectangular mask onto the material surface, while the irradiated target remained stationary. Consequently, only an area of about 2 mm x 2 mm was irradiated during these investigations. Changes in angle of incidence were not mentioned; therefore, irradiation at normal incidence (0°) is assumed. The irradiated alumina surface was "determined by a congruent melting/resolidification process," meaning that the evidence showed that the surface melted under irradiation, with resolidification evident after irradiation. A decrease in the surface roughness in the irradiated region was noted, although the method of measurement was not mentioned. For the high energy regime (> 100 mJ/mm^2), a limiting roughness of 3-5 um on the surface was observed, after a sufficient number of pulses, which was about 50-100 pulses. Lateral flow of the molten material was reported, based upon observations of microsectioned specimens. Microsections also indicated a "planarization," or smoothing, effect and reduction of surface porosity of the irradiated alumina. EDAX-mapping of unirradiated and irradiated areas showed that the Al density, or concentration, after irradiation was higher, which was attributed to a higher overall Al_2O_3 density in the affected surface layer, meaning that the irradiation process increased the density of the affected layer. It was concluded that the formation of a thin molten ceramic layer which flows during irradiation, then solidifies, in combination with ablative material removal, was responsible for the reduction of surface roughness and porosity.

Jagannadham and Narayan (1989) [10] discussed the mechanisms for improvement of fracture strength of excimer laser irradiated ceramics. This discussion was based upon results from previous work by Narayan, et al. [11] and More, et al. [12]. They theorized that the observed increase of bending strength was due to one or more of the following mechanisms:

1. Healing, or welding shut, of surface cracks upon melting and resolidification of the irradiated material.
1. Movement of the surface cracks away from the free surface by the formation of a laser modified region.
1. Laser irradiation forms novel microstructures that introduce compressive stresses in the modified surface region.

Although the research discussed was with ceramics such as Si_3N_4, SiC, and SiC with a thin Ni overlay, the theories stated in this paper may lend insight to strength changes in excimer-irradiated Al_2O_3. Specifically, theories (1) and (2) may complement and agree with the current work, while theory (3) does not seem to agree with the current work. Actually, (3) seems to be the exact opposite conclusion with respect to the current work, as tension stresses in the surface layer may contribute to observed lower bending strength in some instances.

Tonshoff and Gedrat (1989) [13] investigated the interaction of ceramic materials with both KrF (248 nm) and XeCl (308 nm) excimer laser radiation. Fluences up to 500 mJ/mm^2 were investigated. The laser beam was imaged through a rectangular mask and a pair of spherical lenses onto the ceramic surfaces, while the ceramic materials remained stationary during irradiation. Hence, the irradiated areas were very small (< 0.3 mm^2) for any given experiment. No mention of laser beam angle of incidence was made; therefore, perpendicular is assumed. Material removal rates/pulse versus fluence, at a constant 50-Hz pulse frequency, were shown in a graphical form for various ceramics, including Al_2O_3. Fluences from 200-300 mJ/mm^2 were shown to yield sufficient material removal rates. Also, results indicated that these fluences yielded better surface qualities (smoothness) in the irradiated region than lower fluences. It was also stated that although the surface qualities were "very good" in the irradiated zone, the accumulation of condensed reaction products could be a problem. This is in agreement with the current work, as the reaction products were indeed one of the technical challenges faced.

Hontzopoulos and Damigos (1991) [14] investigated changes in surface morphology of tetragonal polycrystalline zirconia (TPZ), partially stabilized zirconia (PSZ), and silicon nitride (Si_3N_4) after irradiation both with an ArF (193 nm) and KrF (248 nm) excimer laser. Angles of beam incidence and whether the samples were moved beneath the beam were not mentioned. Reduction of surface roughness and reduction in porosity were reported, although the methods of measurement and quantifying of these properties were not mentioned. The irradiation-affected surface layer thickness of less than 1 um was reported to increase with fluence, while the uniformity of this layer improved as the number of pulses/unit area increased from 50 to 1000 pulses. Phase changes in the ceramics were also noted. In zirconia, which is normally white, changes in color to a gray or black color were noted. It was concluded that this color change was due the formation of nonstoichiometric oxygen zirconia, dependant upon the oxygen deficiency during irradiation (inert atmosphere or vacuum). Photothermal effects (heating) due to irradiation enhance the mobility of the oxygen atoms, allowing some of the atoms to leave the solid, changing the composition from ZrO_2 to the ZrO_{2-x} phase. Also, in Si_3N_4, the formation of new crystals, after irradiation at a fluence of at least 12 mJ/mm^2, was observed under scanning electron microscopy. It was postulated that these new crystals should be crystalline silicon because Si_3N_4 decomposition starts at 1900° C, a temperature expected on the surface at this fluence.

Furthermore, amorphous silicon is thermodynamically unstable in the presence of crystalline silicon. Thus, when silicon melts, crystal growth is assisted due to the high mobility of the atoms in the liquid phase and the high temperature gradient produced by the laser. It is noted that the temperature in the laser spot could be of the order of 70000 K. The crystallization speed is dependent on the cooling rate, and as the fluence increases, both the temperature and the cooling rate are increased. Interestingly, at fluences greater than 58 mJ/mm^2, these crystals melt and lead to a smooth surface formation. Although the experiments in this work do not include Al_2O_3 irradiation, the theories discussed in this paper, especially the reasons for the formation of new phases, could lend valuable insight to the current work.

Hourdakis and Hontzopoulos (1991) [15] used a KrF (248 nm) excimer laser at fluences up to 130 mJ/mm^2 to affect the surface morphology and properties of bulk Al_2O_3 specimens. The laser beam was imaged onto the sample surface using a 100-mm focal length cylindrical lens, while moving the workpiece by means of a stepper motor, similar to the current work. Tilting the substrates with respect to the laser beam was not mentioned. It is assumed that all work was done at normal incidence. It was reported that the results indicated a reduction of surface roughness, porosity, and density of microcracks, although no method of quantifying these qualities was mentioned. It was reported that the ceramic surface roughness value decreased as the fluence was increased up to about 60 mJ/mm^2, but then increased as the fluence increased, as a result of material removal. X-ray diffraction analysis revealed a phase transformation induced by the laser irradiation at fluences greater than 60 mJ/mm^2 in the near-surface region of the stable, hexagonal, alpha-alumina to the meta-stable, cubic, gamma-alumina phase. The data showed that the formation of the gamma-alumina depended directly upon the number of pulses per unit area. Larger gamma peaks were evident on the X-ray diffraction analysis spectrum as the pulse counts increased from 50, 100, 500, and 1000 pulses per unit area.

Bergmann, et al., (1991) [16] reported on the interaction of pulsed XeCl (308 nm) excimer laser radiation with ceramic surfaces. Imaging of the laser beam onto the surface using the mask projection technique was used. No mention of specimen motion or variation of the beam angle of incidence was made. A summary of possible technological applications, specifically, improving the tensile strength of Au, Cu, and Ni lead frame bonds, laying bare of graphite in iron, and improving the wear resistance of Al_2O_3 substrates, was discussed. Most notably, it was stated that irradiation-affected melt depth of any given material is predominately influenced by its thermal conductivity and this, in turn, will be the controlling factor in surface modification. If the material has a high thermal conductivity, the laser

power is quickly transferred into the bulk volume by thermal conduction. This results in increased roughness, as the melt zone does not exist long enough to allow thermal flow processes to occur. Conversely, by the same principle, surface roughness reduction of materials with low thermal conductivity can be obtained. The increase of the Weibull modulus [17] of Al_2O_3 by excimer irradiation was also reported. A fluence of 30 mJ/mm^2 and 35 pulses/unit area increased the Weibull modulus of 96% alumina from the as-fired value of m=7.8, to a post-irradiated value of m=16, while the mean strength of the irradiated samples decreased with respect to the unirradiated samples. Ninty-eight percent and 99.7% alumina substrates showed similar Weibull modulus values, although no as-fired values for these materials were reported.

Schubert, et al., (1991) [18] reported on the effect of excimer laser irradiation on 96%, 98%, 99.7% as-fired Al_2O_3 substrates and 99.7% Al_2O_3 mechanically polished substrates, with respect to surface roughness, tensile strength, and Weibull modulus (m). The mask projection technique was used with both 193-nm and 351-nm wavelength lasers, although which laser was used for which experiment was not given. Fluences of 30-40 mJ/mm^2 and up to 40 pulses/unit area were reported to give favorable results on surface roughness, based upon qualitative scanning electron microscopy evaluation. The Weibull modulus of nearly all samples tested increased significantly upon excimer irradiation with respect to the as-received conditions (see Table 1). The tensile strength at 10% probability of failure showed improvement for the 96% and 98% alumina substrates under all conditions tested (30-40 mJ/mm^2, 16-32-35 pulses/unit area), while the 99.7% alumina tensile strength decreased slightly.

Table 1. Weibull Modulus (m) Values of Al_2O_3, From Schubert, *et al. [18]*

% Al_2O_3	As-Received	30 mJ/mm^2 35 pulses	40 mJ/mm^2 16 pulses	40 mJ/mm^2 32 pulses
96%	m=7.8	m=16	m=12.8	N/A
98%	m=11.0	m=14.9	m=15.1	N/A
99.7%	m=11.0	m=16.2	N/A	m=18.5
99.7% polished	m=12.6	m=10.9	N/A	m=22.2

Lowndes, et al. (1992) [2] examined the effects of XeCl excimer laser irradiation (308 nm) on as-received polycrystalline 99.6% Al_2O_3 and mechanically polished, single-crystal Al_2O_3 (sapphire), as a function of laser fluence. The laser beam was imaged through a rectangular aperture and a spherical lens onto the stationary target surfaces. Angle of incidence was not mentioned, but it is assumed to be normal. Results showed that at low to moderate fluences (< 60 mJ/mm^2), both materials were affected by the laser radiation only after some number of incubation pulses. This number was much larger for the single-crystal sapphire than for the polycrystalline Al_2O_3, but decreased with increasing fluence for both materials. Laser etch (material removal) rates were similar for both materials, after the incubation period. Scanning electron micrographs were interpreted as indicating that the alumina melts and flows

after irradiation at fluences as low as 7 mJ/mm^2, after a sufficient number of incubation pulses, although the melting is somewhat nonuniform at this fluence level. Significant qualitative reduction of surface roughness was reported for the polycrystalline alumina after sufficient pulses at fluences of 10-30 mJ/mm^2. To better characterize the nature of the incubation phenomena, time-resolved measurements of ion currents in the plasma plume of material emitted from the Al_2O_3 were conducted. These tests were carried out in a vacuum, under 248 nm, 11 mJ/mm^2, excimer irradiation. The ion probe measurements of ion currents in the plasma plume showed that the number of ions emitted from the alumina increased up to a saturation level after about 50 laser pulses. Plume velocities were reported to increase with the number of successive pulses, up to a saturation level at about 10 pulses, where the velocity was observed to be 20,000-30,000 m/sec, helping to confirm the incubation phenomena. It was suggested that the incubation pulses apparently damaged the Al_2O_3 substrates, making defects or absorption centers, which made the substrates more energy-absorbing by successive laser pulses. These defects may be either the grain boundaries in the polycrystalline Al_2O_3 substrates, or, as stated previously, can be laser-generated, hence, the reason for the incubation time being longer in the sapphire. It was concluded that a sufficient concentration of laser-generated defects, or absorption centers, was necessary before efficient material removal could occur.

Activity

Development of Laser System

The laser system used in this study was custom designed and built by procuring the separate subsystems (laser, gas handling equipment, beam delivery system, etc.) and integrating them to form a system that would allow versatility in experimenting with several different laser applications, while addressing the safety concerns such as the laser beam and the halogen gas that is used in the laser. The equipment for the system was procured in 1988. At that time there were no commercially available assembled excimer systems that met all requirements.

The laser system used in this study is based on a Questek model 2860 excimer laser [19], capable of sustaining 500 mJ/pulse at 50 Hz with a KrF gas mixture (248 nm). The KrF gas mixture was chosen over the other gas mixtures due to the higher power output available with KrF. Also, this wavelength is absorbed well by alumina. The additional equipment that completes the system includes the following:

- Halogen gas handling system, which includes gas cabinet, halogen gas monitors, and electro-pneumatic gas controller.
- Room air halogen gas scrubber, for containing and cleaning up any gas leaks.
- Cryogenic halogen gas processor, for cleaning laser gas of contaminants.
- Beam delivery system consisting of optical rail, excimer optics, and mask holder.
- Custom 8-axis motion control system, including stepper motors, personal computer, and computer/stepper motor interface.
- Polycarbonate class 1 laser enclosure.
- Two sturdy tables on which to mount the laser and beam delivery system.

- The laser was mounted and leveled on one of the tables, while the second table was placed on the output end of the laser. The beam delivery system was mounted on this second table, leveled

and aligned so that the laser beam would travel along the rail. The 8-axis motion control system was installed with the stepper motor controlled tables in place to handle the job of moving the optics, mask holder, and target station. The stepper motors in the 8-axis motion control system were linked to the personal computer to provide computer numerical control (CNC) over the system. Additionally, the computer was interfaced to the laser, to provide programmable control of laser ON/OFF. The polycarbonate class 1 laser enclosure was installed over the laser beam path, to ensure safety to the laser operator with respect to direct, stray, or scattered radiation. This enclosure had a hinged hood over the beam delivery system to allow access to the optics, mask holder, and target holder. The hood was interlocked to the laser, to shut the laser off in case of enclosure opening, as an added safety consideration to personnel.

The gas handling equipment was installed and plumbed to the laser to handle the gases in the system: argon, krypton, helium, neon, and 5% fluorine in helium. A 316 stainless steel piping was used on all gas lines, due to its strength and noncorrosive properties. The laser gas cabinet was vented to an exhaust fan, with halogen scrubbers in-line, to prevent halogen leaks into the laser room. Halogen gas detectors were installed near the laser and inside of the gas cabinet. These detectors were wired into the electro-pneumatic gas controller, which would close a pneumatic valve on the halogen gas bottle in case of a leak, fire, loss of power, etc. The room air halogen gas scrubber was installed over the laser, suspended from the ceiling, and wired into the electro-pneumatic controller. This scrubber was designed to turn on in case of a halogen leak detected by system. This was an added measure of safety for personnel in the laser room.

The cryogenic gas processor was connected to the laser chamber. This is a closed loop system that pumps the laser gas mixture from the lasing chamber, through the cryogenic processor, through a particulate filter, then back into the lasing chamber. Without such a system, laser-generated contaminants would quickly build up and quickly destroy the internal optics and electrode assembly.

Finally, this laser system was installed in an enclosed, locking room, for both safety and security concerns. A photograph of the system is shown in Figure 1.

Characteristics of As-Received Alumina

Thin film substrates of 99.6% alumina content (polycrystalline, *alpha*-Al_2O_3), 95 mm x 114 mm size, and 0.25 mm thickness (commercial designation ADS-996 [1]) were used in this study. The surface finish of the substrates, measured by digital interferometer, was found to be 475 nm (mean). The average grain size was reported to be 1.2 um [1]. The mean flexural strength, determined by the four-point bend method, was found to be 550 MPa. The Weibull modulus was 9.1.

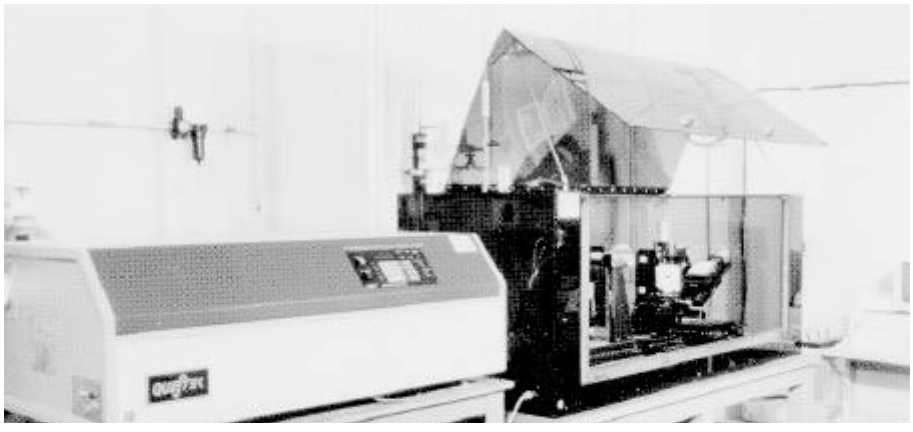

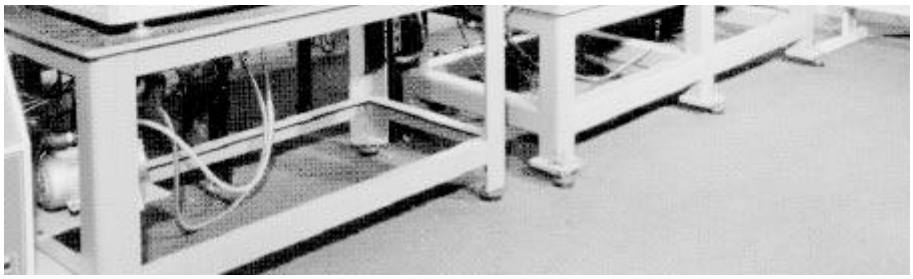

Figure 1. Laser System

Irradiation Procedure

The substrates were irradiated in air with an excimer laser emitting pulses at 248-nm wavelength, with 20-ns pulse duration, and pulse frequency set at a constant 50 Hz. The laser beam was masked to reduce the beam size from 22 mm x 11 mm, to 17 mm x 9 mm, in order to obtain uniform radiation density. The beam was passed though a 200-mm focal length cylindrical lens and focused near the substrates surface, yielding an effective normal beam size of 17 mm x 0.1 mm. This produced a maximum fluence of 125 mJ/mm^2 on the substrate surface, perpendicular to the laser beam, while the laser was operating at 500 mJ/pulse. The fluence was varied by changing the laser energy output.

The surface to be treated was moved below the beam on an X-Y computer-controlled table. Because the laser was pulsed at a constant 50 Hz, the number of laser pulses/unit area was controlled by the table speed. For instance, this would result in a laser pulse every 25.4 um of table travel at a table speed of 76.2 mm/minute, resulting in 8 pulses/unit area. A slower table speed would result in a higher pulse density, while a faster table speed would result in a lower pulse density.

The X-Y table could also be rotated about a horizontal line perpendicular to the beam path, allowing the sample to be tilted at various angles of incidence (θ) with respect to the laser beam. θ (theta) is defined as the angle measured from the plane perpendicular (normal) to the laser beam, to actual plane of the substrate during the irradiation process. For instance, a θ of 0° would equate to normal incidence between the laser beam and the substrate, while a θ of 90° would place the substrate parallel to the beam path. Figure 2 illustrates this relationship.

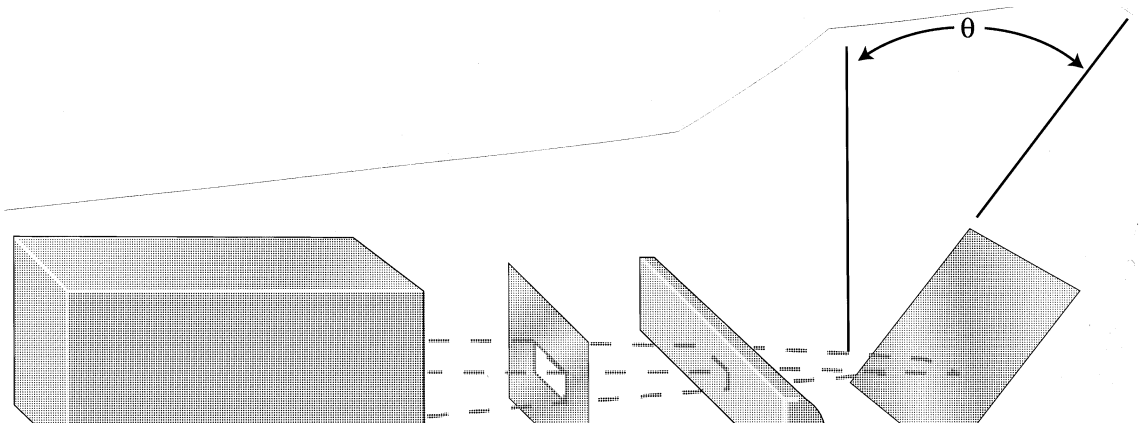

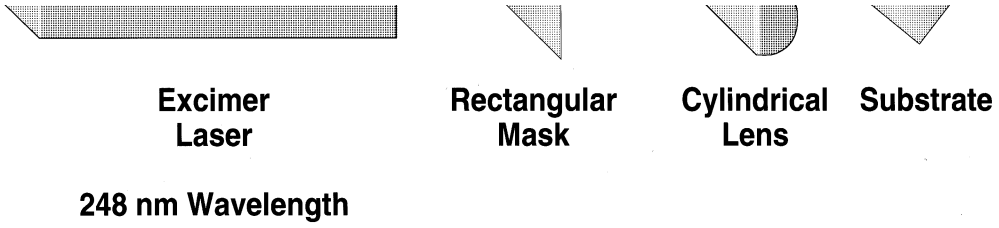

Figure 2. Schematic of Laser System

Post-Irradiation Thermal Treatment Procedure

Post irradiation thermal treatments (sintering) were conducted in air. The time at temperature, peak temperature, and ramp rate of the furnace were computer controlled.

Assessment Techniques

A contact-type surface profiling system was used early in this project to quantify the surface roughness of the irradiated specimens. The contact-type system was judged inferior to the interferometric system, discussed later, as the stylus tip radius (5.1 um) was much too large to give a true profile of the measured surfaces. For this reason it was abandoned.

A WYCO TOPO 2-D digital interferometric, noncontact, surface profiling system was used to quantify the surface finish of the specimens [20]. A spatial sampling interval of 0.65 um over a scan length of approximately 655 um was used. A minimum of three scans on each sample was used to ensure a true representation of the surface. The surface roughness was quantified using the center line average (CLA), or roughness average (R_a) [21].

A four-point bend test, conforming to ASTM C 158, was used to measure flexural strength [22]. The substrates were scribed 40% of the substrate thickness on the backside with a Nd:YAG laser, to size of 50.8 mm x 5.1 mm. The substrates were then snapped and separated into individual bend test specimens. The opposite (front) surfaces were irradiated, then stressed in tension during the four-point bend test. The tests were conducted using an Instron universal test machine.

Transmission electron microscopy (TEM), scanning electron microscopy (SEM), and X-ray diffraction (XRD) were used to examine the surfaces of the irradiated specimens. Taper-sectioning was used to observe the depth and structure of the radiation-affected layer. The transmission electron microscopy

services and results were provided by the Analytical Sciences laboratory at AlliedSignal Federal Manufacturing & Technologies. The X-ray diffraction services were arranged by contract through AlliedSignal Analytical Sciences Laboratory, Morristown, New Jersey.

Results

Effects of Irradiation

Effect on Surface Layer: Figure 3 shows two separate irradiated areas on a substrate upon being

subjected to (3a) one laser pulse, and (3b) two consecutive laser pulses, at a fluence of 125 mJ/mm^2 and an angle of 60° . After one pulse, many of the surface grains show evidence of being melted and flowed (3a). After two pulses (3b), the substrate appears to be a smooth, closed surface with the underlying grains almost completely covered by the flowed material. Fine particles (<< 1 um) appear on the surface of both areas.

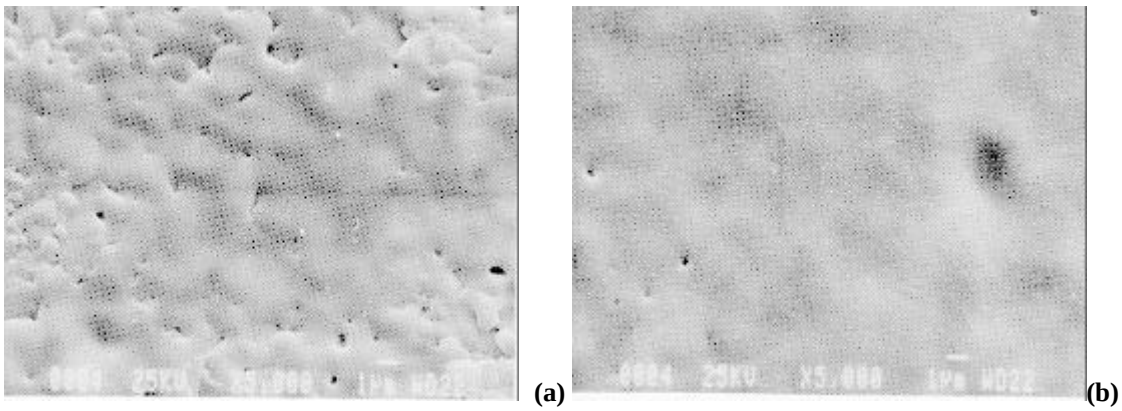

Figure 3. 99.6% Alumina Surface After 1 (a) and 2 (b) Laser Pulses

Figure 4 shows SEM photographs of an irradiated specimen taper-sectioned at an angle of about 10° . The specimen was irradiated at an angle of incidence of 60° , a fluence of 125 mJ/mm^2, and a pulse density of 8 pulses/unit area. The affected layer appears to be dense with little porosity and has an average depth of 2 um.

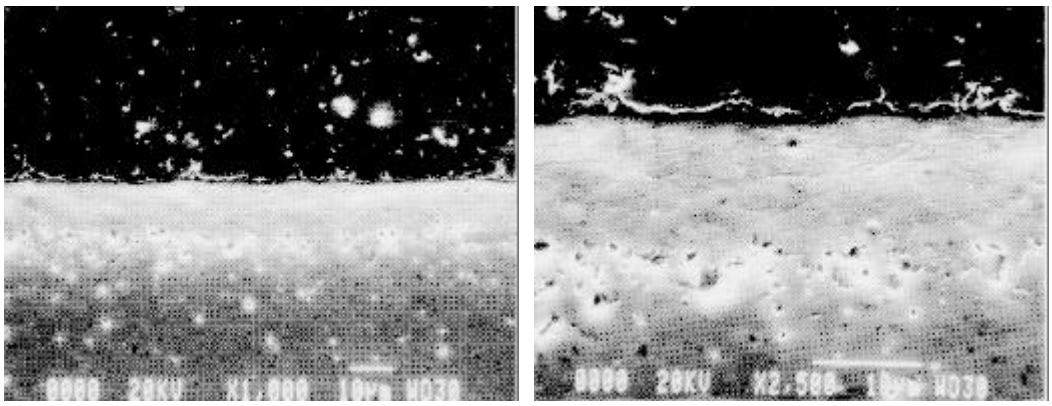

Figure 4. Taper-Section of Irradiated Alumina at θ = 60° , 125 mJ/mm^2, 8 Pulses/Unit Area

A fine particulate, deposited on the laser track under all irradiation conditions, was partially adherent and could be somewhat wiped off the irradiated surface by a gloved finger. The particulate appeared as a fine white powder on the finger. This particulate was found to impair the adhesion of vacuum-deposited metal films onto the substrates, as the metal would coat the particulate, not the bulk substrate, allowing the metal to be removed with the particulate by wiping with a finger. Figure 5 shows scanning electron microscope photographs of the particulate that was removed by adhesive tape from an irradiated substrate surface. Note what appears to be very small grains in this particulate.

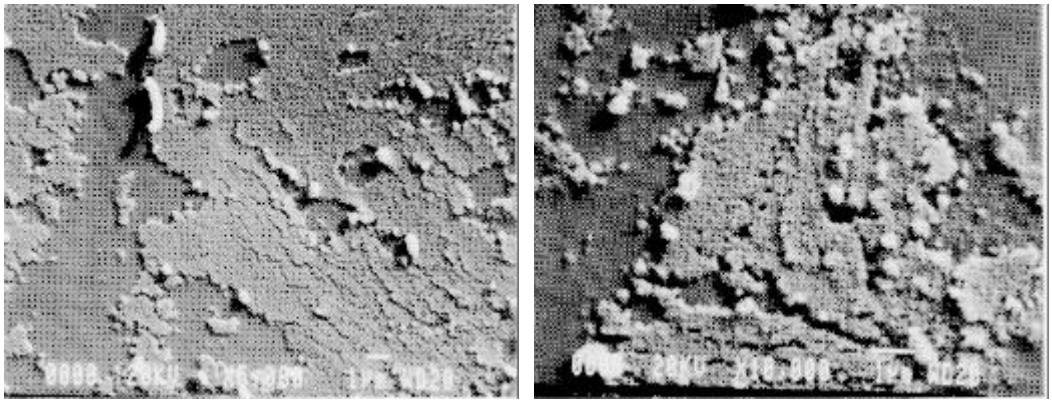

Figure 5. Irradiation-Generated Particulates

Transmission electron microscopy and X-ray diffraction results suggest that the particulate contains gamma-alumina, along with alpha-alumina, and spinel ($MgAl_2O_3$). (Gamma-alumina is a phase of alumina that is at this time a matter of discussion as far as its true nature. The two main differences are that alpha-alumina is a hexagonal structure and stable, while gamma is cubic and meta-stable [23].)

For transmission electron microscopy (TEM) examination, samples of the particulate were extracted from the irradiated surface by two methods. The first method was to gently pull a carbon-coated 100-mesh Formvar substrate copper grid over the irradiated surface. The second method was to lightly scrape the irradiated surface with a new razor blade and collect the scrapings on grids. The second method yielded more material than the first method. Five different selected area electron diffraction patterns (SADPs) were analyzed by a transmission electron microscope at an operating voltage of 200 kV . SADPs of samples extracted from the surface consisted of diffuse, concentric rings, indicating the presence of many randomly oriented fine particles. The ring diameters were measured using a Supper diffraction pattern reader with a precision of 0.05 mm. All five SAPDs yielded a consistent series of interplanar spacings. Appendix B contains two analyses by this method, labeled plate 1640 and plate 1643. Plate 1640 was acquired using the first extraction method, while plate 1643 was acquired using the second method. From the set of interplanar spacing derived, the crystal structures were narrowed to 16 possible alumina structures known to exist in the Joint Committee on Powder Diffraction Standards files. Based on the intensity of the diffraction rings and the ability to assign a consistent set of interplanar spacings to each observed line, it was concluded that the structure of the fine particles was that of *gamma* and *alpha*-alumina. The diffraction patterns showed broad diffuse rings. This line broadening was measured and, by dividing the electron wavelength at 200 kV (0.0251 A) by the ring broadening (0.000281 radians), the breadth of the rings was used to calculate an average particle size of 9 nm.

X-ray diffraction (XRD) patterns of irradiated samples were obtained on a Rigaku diffractometer. Appendix C contains two copies of the patterns. Pattern 1 contains peaks that were assigned to spinel ($MgAl_2O_3$) and *gamma*-alumina. Pattern 2 compares the irradiated surface to the as-received surface. Three peaks exist on the patterns that can be attributed to *gamma*-alumina.

Effect on Surface Roughness: Figure 6 compares the surfaces of an as-received 99.6% Al_2O_3

substrate (6a) with both a mechanically polished 99.6% Al_2O_3 [1] substrate (6b) and a substrate irradiated (6c) at an angle of incidence of 60° , a fluence of 125 mJ/mm^2, and 8 pulses/unit area. Note the relative smoothness of the irradiated surface, compared with the as-received material. Also note the grain pullouts in the mechanically polished material. Scanning electron microscopy examination at 2000X magnification was performed on both the mechanically polished and irradiated surfaces in an attempt to quantify and compare the defect count/unit area. Only defects measuring a minimum of 1 um, measured across the widest point, were counted. Three separate areas were observed on each surface. The mechanically polished material averaged 16 defects/mm^2, while the irradiated material averaged less than 1 defect/mm^2.

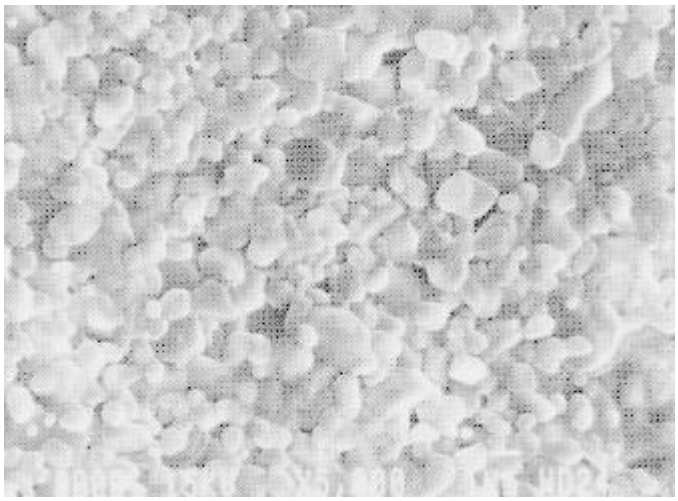

(a) As-received

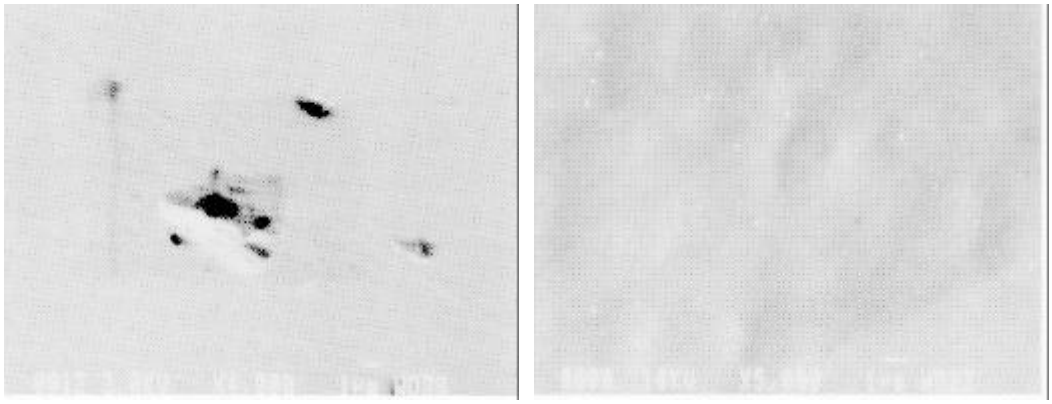

(b) Mechanically Polished (c) Irradiated

Figure 6. Typical Substrate Surfaces

Figure 7 gives profile scans of an as-received substrate (7a), a mechanically polished substrate (7b), and a substrate irradiated (7c) at an angle of incidence of 60° , a fluence of 125 mJ/mm^2, and 8 pulses/unit area. The R_a values derived from the measurements of the as-received, the mechanically polished, and the irradiated samples were 450 nm, 6.9 nm, and 46.6 nm, respectively.

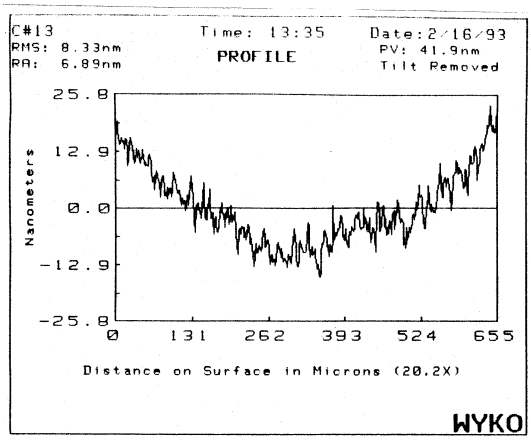

(a) As-received

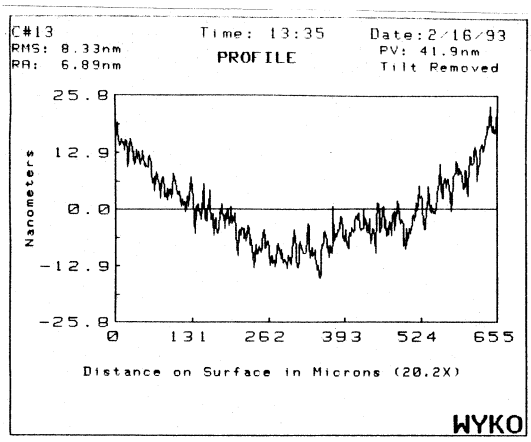

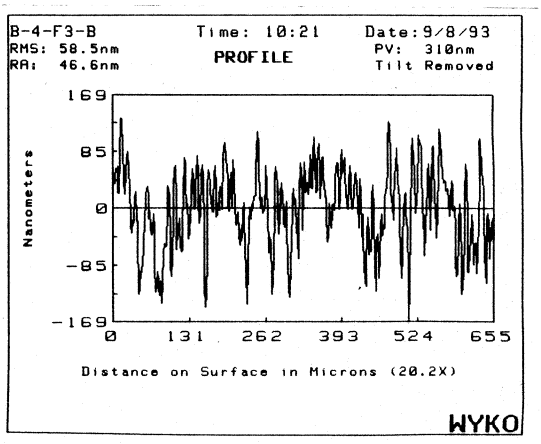

(b) Mechanically Polished (c) Irradiated

Figure 7. Comparison of Surface Profile Scan Results

Early profilometry results comparing surfaces irradiated at various angles of incidence (0° , 30° , 45° , and 60°), pulses densities (4, 8, and 16 pulses/unit area), and two separate fluence levels (87 and 125 mJ/mm^2), suggested that 125 mJ/mm^2 fluence yielded lower surface roughness values (R_a) than 87 mJ/mm^2 fluence. Three samples at each fluence level and angle of incidence, one at each pulse density, were measured in this experiment. The data from this experiment is located in Appendix D. Table 2 is a summary of the results from this experiment. Based on this data, it was decided that the remainder of the research would be conducted at a fluence of 125 mJ/mm^2, in part to limit the amount of data gathering necessary for this project.

Table 2. Comparison of Surface Roughness for Two Fluence Levels

Angle of Incidence (degrees)	Fluence (mJ/mm^2)	Average R_a (nm)
0	87	316
	125	284
30	87	293
	125	243
45	87	150
	125	103
60	87	132
	125	65

Figure 8 illustrates the effect of varying the beam angle of incidence and the number of pulses/unit area on mean R_a values for irradiation at a fluence of 125 mJ/mm^2. For comparison, the as-received ceramic had an average R_a of 457 nm, with a range of 234-842 nm, while the best mean R_a results obtained after laser treatment was 60 nm, with a range of 51-74 nm. The data from this experiment is located in Appendix E.

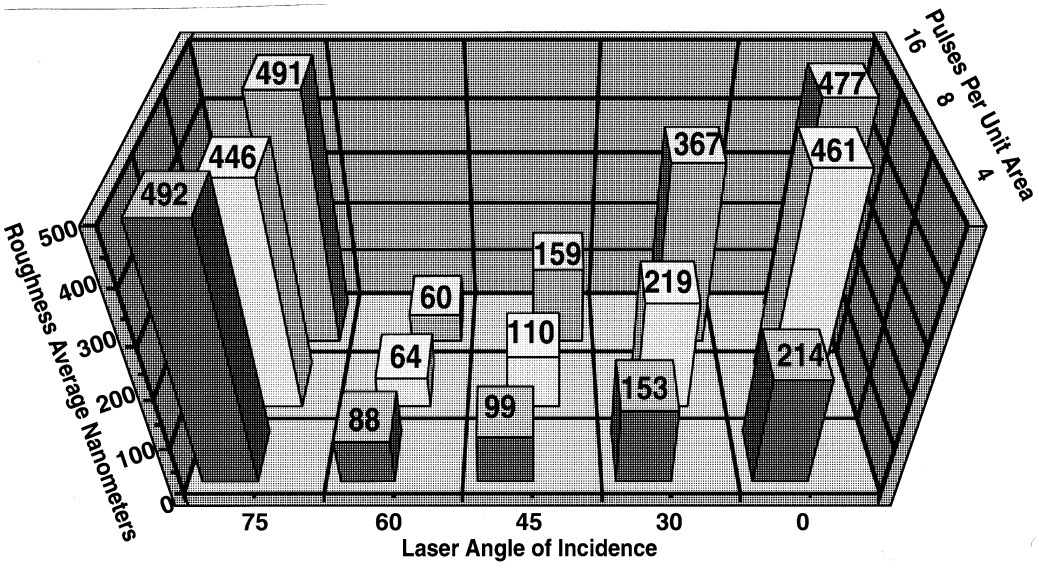

Figure 8. Effect of Incident Angle and Number of Pulses/Area on Average Surface Roughness

An experiment was designed to determine whether the decrease in surface roughness after irradiation could be attributed to either (1) some mechanism dependent on the angle of incidence or (2) the fact that tilting the workpiece to the laser beam at some angle other than normal simply increases the illuminated area. For instance, an angle of incidence of 60° doubles the area illuminated by the laser on the workpiece, effectively halving the average fluence.

Group 1, consisting of seven specimens, was irradiated by a beam size of 0.1 mm x 16.5 mm at a fluence of 125 mJ/mm^2 (measured in a plane perpendicular to the laser beam) and an angle of incidence of 60° . This resulted in an average fluence of 62.5 mJ/mm^2 in a laser spot size of 0.2 mm x 16.5 mm, measured along the substrate surface. Laser pulse frequency was set at 50 Hz and the table speed used was 76.2 mm/min, which resulted in a pulse density of 8 pulses/unit area on the substrate surface.

Group 2, also seven specimens, was irradiated by a beam size of 0.1 mm x 16.5 mm, at a fluence of 62.5 mJ/mm^2 and an angle of incidence of 0° (perpendicular). Laser pulse frequency was 50 Hz, while the table speed used was 38.1 mm/min, resulting in a pulse density of 8 pulses/unit area on the substrate surface.

This experiment compares two surfaces subjected to the same total amount and deposition rates of laser energy/unit area. The average fluence, pulse frequency, and the pulse density of the two groups were the same, with the only variable being the laser beam angle of incidence. The two groups were evaluated by interferometric surface profile measurements. The surface roughness average (R_a) results are below.

Group 1 $\theta = 60^o$ Group 2 $\theta = 0^o$

R_a= 54 nm R_a= 177 nm

51 238

62 140

58 159

117 248

46 101

64 233

Ave.= 64 nm Ave.= 192 nm

Effect on Flexural Strength: Four-point bend tests were conducted on irradiated specimens. Some of the same laser parameters used previously for surface finish investigations were applied to the 4-point bend samples, because this was not an attempt to optimize the irradiation process for strength improvement in alumina, but to simply determine what changes the irradiation had on the strength of the substrates.

The experimental data consist of breaking loads, in pounds-force (lbf), for each of several specimens. This data was then used to calculate the bending strength, or modulus of rupture, for each specimen. The modulus of rupture is defined as the value of maximum tensile stress in the extreme fiber of a beam loaded to failure in bending, computed from the flexure formula [22]:

$$S_b = \frac{Mc}{I}$$

where:

S_b = modulus of rupture in bending,

M = maximum bending moment, computed from the maximum load and the original moment arm,

c = initial distance from the neutral axis to the extreme fiber where failure occurs, and

I = initial moment of inertia of the cross section about the neutral axis.

Calculation for modulus of rupture for specimens of rectangular cross-section is [22]:

$$S = \frac{3La}{bd^2}$$

where:

S = modulus of rupture, psi (MPa),

L = breaking load, lbf (N),

a = separation of adjacent loading and support edges, in. (mm),

b = width of specimen, in. (mm), and

d = thickness of specimen, in. (mm)

The results were analyzed using Weibull statistics [17]. Figure 9 is a Weibull plot comparing the as-received condition to samples irradiated at angles of incidence of 30° and 60° , 8 pulses/unit area, and a fluence of 125 mJ/mm^2. Appendix F contains the data from this experiment and a sample bending strength calculation.

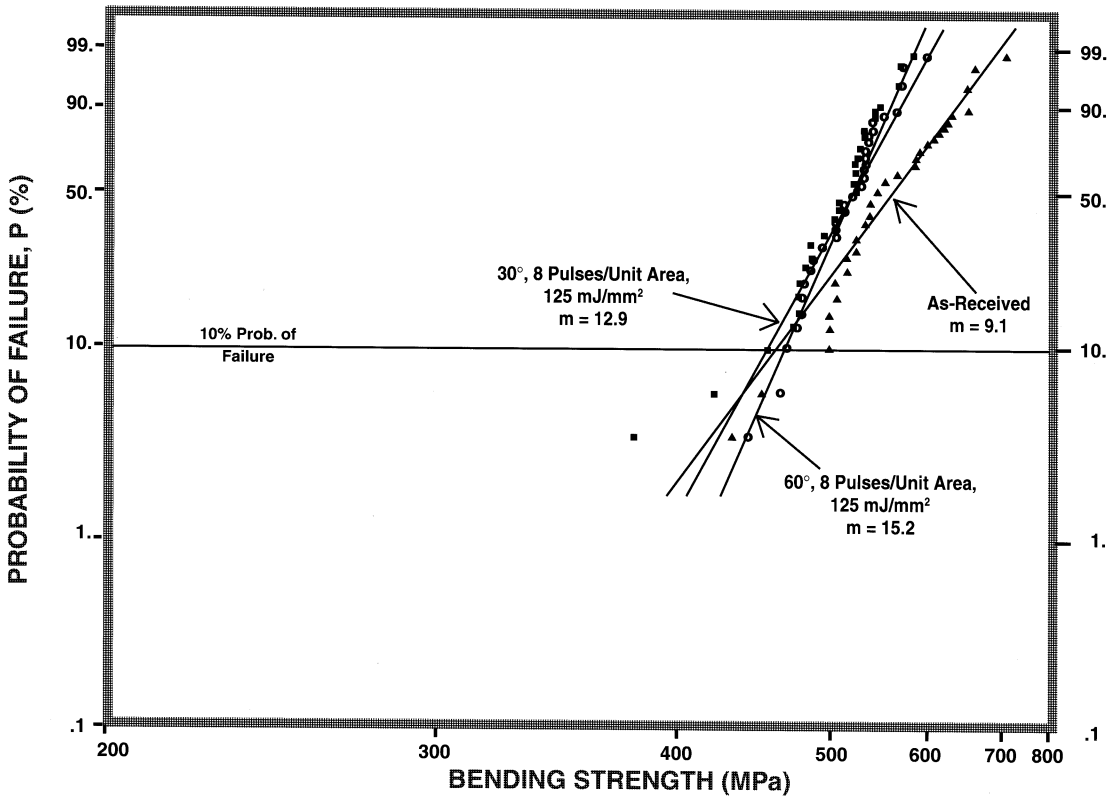

Figure 9. Weibull Plot of As-Received Versus Irradiated Alumina

Effects of Post-Irradiation Thermal Treatment

Effect on Surface Layer: Several methods and solvents were tried in attempts to remove the particulate from the surface after irradiation, including ultrasonic cleaning; washing with xylene, alcohols, trichloroethylene, and surfactants; abrasion with polishing media; HF and HCl acid treatment; high-pressure washing; and vapor blasting. Results showed that the a portion of the particulate either adhered to the substrate or the substrate surface was degraded by the cleaning method. None of the methods tried gave adequate results. Figure 10 shows typical substrate surfaces after (10a) HF bathing and (10b) abrasion by a fine polishing media. On the specimen that went through the HF bath, there was evidence of particulate remaining on the surface after cleaning and the scanning electron photograph shows evidence of surface grain boundary etching. The specimen that was subjected to the abrasion cleaning also had particulate remaining on the surface after treatment.